

HYCOT: HYPERSPECTRAL COMPRESSION TRANSFORMER WITH AN EFFICIENT TRAINING STRATEGY

Martin Hermann Paul Fuchs¹, Behnoor Rasti^{1,2}, Begüm Demir^{1,2}

¹Faculty of Electrical Engineering and Computer Science, Technische Universität Berlin, Germany

²BIFOLD - Berlin Institute for the Foundations of Learning and Data, Germany

ABSTRACT

The development of learning-based hyperspectral image (HSI) compression models has recently attracted significant interest. Existing models predominantly utilize convolutional filters, which capture only local dependencies. Furthermore, they often incur high training costs and exhibit substantial computational complexity. To address these limitations, in this paper we propose Hyperspectral Compression Transformer (HyCoT) that is a transformer-based autoencoder for pixelwise HSI compression. Additionally, we introduce an efficient training strategy to accelerate the training process. Experimental results on the HySpecNet-11k dataset demonstrate that HyCoT surpasses the state-of-the-art across various compression ratios by over 1 dB with significantly reduced computational requirements. Our code and pre-trained weights are publicly available at <https://git.tu-berlin.de/rsim/hycot>.

Index Terms— Image compression, hyperspectral data, deep learning, transformer, efficient training, remote sensing.

1. INTRODUCTION

Hyperspectral sensors acquire images with high spectral resolution, producing data across hundreds of observation channels. This extensive spectral information allows for detailed analysis and differentiation of materials based on their spectral signatures. However, the large number of spectral bands in hyperspectral images (HSIs) presents a significant challenge, namely the vast amount of data generated by hyperspectral sensors. While the volume of hyperspectral data archives is growing rapidly, transmission bandwidth and storage space are expensive and limited. To address this problem, HSI compression methods have been developed to efficiently transmit and store hyperspectral data.

Generally, there are two categories of HSI compression: i) traditional methods [1–3]; and ii) learning-based methods [4–8]. Most traditional methods are based on transform coding in combination with a quantization step and entropy coding. In contrast, learning-based methods train an artificial neural network (ANN) to extract representative features and

reduce the dimensionality of the latent space via consecutive downsampling operations.

Recent studies indicate that learning-based HSI compression methods can preserve reconstruction quality at higher compression ratios (CRs) compared to traditional compression methods [9]. Thus, the development of learning-based HSI compression methods has attracted great attention. The current state-of-the-art in this field is formed by convolutional autoencoders (CAEs) [4–6]. The 1D-Convolutional Autoencoder (1D-CAE) model presented in [4] compresses the spectral content without considering spatial redundancies by stacking multiple blocks of 1D convolutions, pooling layers and leaky rectified linear unit (LeakyReLU) activations. Although high-quality reconstructions can be achieved with this approach, the pooling layers limit the achievable CRs to 2^n . Another limitation of this approach is the increasing computational complexity with higher CRs due to the deeper network architecture. Unlike [4], to achieve spatial compression, Spectral Signals Compressor Network (SSCNet) that focuses on the spatial redundancies via 2D convolutional filters is introduced in [5]. In SSCNet, compression is achieved by 2D max pooling, while the final CR is adapted via the latent channels inside the bottleneck. With SSCNet much higher CRs can be achieved at the cost of spatially blurry reconstructions. To achieve joint compression of spectral and spatial dependencies, 3D Convolutional Auto-Encoder (3D-CAE) is introduced in [6]. 3D-CAE applies spatio-spectral compression via 3D convolutional filter kernels. Residual blocks allow gradients to flow through the network directly and improve the model performance. In general, CAEs fail to capture long-range spatial and spectral dependencies and their stacked convolutional layers make the architectures computationally expensive.

It is important to note that deep learning models require large training sets to effectively optimize their parameters during training. On the one hand, training deep learning models on these large training sets allows them to generalize well. On the other hand, training often requires hundreds of epochs for model weight convergence [10], which results in high training costs. While training time can be reduced through parallelization on multiple GPUs, energy consumption and hardware requirements are still limiting factors.

To address these problems, we propose a transformer-based autoencoder for HSI compression, named HyCoT. HyCoT leverages long-range spectral dependencies for latent space encoding. For fast reconstruction, HyCoT employs a lightweight decoder. To accelerate training while maintaining reconstruction quality, we propose an efficient training strategy that reduces the training set size. Experimental results demonstrate that HyCoT achieves higher reconstruction quality across multiple CRs, while reducing both training costs and computational complexity compared to state-of-the-art methods.

2. METHODOLOGY

Let $\mathbf{X} \in \mathbb{R}^{H \times W \times C}$ be an HSI with image height H , image width W and C spectral bands. The objective of lossy HSI compression is to encode \mathbf{X} into a decorrelated latent space $\mathbf{Y} \in \mathbb{R}^{\Sigma \times \Omega \times \Gamma}$ that represents \mathbf{X} with minimal distortion $d : \mathbf{X} \times \hat{\mathbf{X}} \rightarrow [0, \infty)$ after reconstructing $\hat{\mathbf{X}} \in \mathbb{R}^{H \times W \times C}$ on the decoder side.

To efficiently and effectively compress \mathbf{X} , we present HyCoT. HyCoT is a learning-based HSI compression model that employs the SpectralFormer [11] as a feature extractor on the encoder side, and a lightweight multilayer perceptron (MLP) for lossy reconstruction on the decoder side. Our model is illustrated in Figure 1. In the following subsections, we provide a comprehensive explanation of the proposed model.

2.1. HyCoT Encoder

The HyCoT encoder $E_\Phi : \mathbf{X} \rightarrow \mathbf{Y}$ uses the SpectralFormer [11] as a backbone for spectral feature extraction. It aggregates long-range spectral dependencies via transformer blocks [12] inside a compression token (CT) and then projects the CT into the latent space using an MLP to fit the desired target CR.

In detail, each pixel \mathbf{x} of \mathbf{X} is processed separately. First, spectral groups \mathbf{g}^i are formed by nonoverlapping grouping of g_d neighbouring spectral bands, where g_d denotes the group depth. To make the number of bands divisible by g_d , \mathbf{x} is padded from C to $C_{\text{pad}} = C + \Delta_{\text{pad}}$, forming \mathbf{x}_{pad} , where $\Delta_{\text{pad}} = g_d - C \bmod g_d$. The spectral groups are linearly projected to the embedding dimension d_{emb} using a learnable matrix \mathbf{P} . The resulting embedding vectors (so-called tokens) are defined as $\tilde{\mathbf{t}}^i = \mathbf{P}\mathbf{g}^i$. We propose prepending a learnable CT $\tilde{\mathbf{t}}^0$, which is also encoded by the transformer encoder to capture the spectral information of the pixel. The overall number n_t of tokens per pixel thus equals $n_t = C_{\text{pad}}/g_d + 1$. Afterwards, a learned position embedding \mathbf{l}^i is added to the patch embeddings to retain the positional information of the spectral groups as $\mathbf{t}^i = \tilde{\mathbf{t}}^i + \mathbf{l}^i$.

The sequence of tokens is then fed into the transformer encoder that stacks L transformer blocks. At each transformer

block $l = 1, \dots, L$, multi-head self-attention (MSA) is applied followed by an MLP [12]. For both, a residual connection [13] is employed, followed by a layer normalization (LN) [14]:

$$\mathbf{t}'_l = \text{MSA}(\text{LN}(\mathbf{t}_{l-1})) + \mathbf{t}_{l-1}, \quad (1)$$

$$\mathbf{t}_l = \text{MLP}(\text{LN}(\mathbf{t}'_l)) + \mathbf{t}'_l, \quad (2)$$

where MSA is an extension of self-attention (SA) that runs k self-attention operations (heads) in parallel and projects their concatenated outputs [12]:

$$\text{MSA}(\mathbf{t}) = [\text{SA}_1(\mathbf{t}); \text{SA}_2(\mathbf{t}); \dots; \text{SA}_k(\mathbf{t})] \mathbf{U}_{\text{MSA}}. \quad (3)$$

SA computes a weighted sum over all values \mathbf{v} for each token \mathbf{t} and the attention weights \mathbf{A}_{ij} are based on the pairwise similarity between the query \mathbf{q}^i and key \mathbf{k}^j of two respective tokens [12]:

$$[\mathbf{q}, \mathbf{k}, \mathbf{v}] = \mathbf{t} \mathbf{U}_{\text{qkv}}, \quad (4)$$

$$\mathbf{A} = \text{softmax} \left(\frac{\mathbf{q}\mathbf{k}^T}{\sqrt{d_{\text{emb}}/k}} \right), \quad (5)$$

$$\text{SA}(\mathbf{t}) = \mathbf{A}\mathbf{v}. \quad (6)$$

The CT is extracted and sent to the MLP encoder that adapts the latent space channels Γ to fit the target CR. HyCoT compresses only the spectral content, and therefore the CR can be simplified as follows:

$$\text{CR} = \frac{C}{\Gamma}. \quad (7)$$

The MLP encoder initially applies a linear transformation of the CT with the embedding dimension d_{emb} to a hidden dimension d_{hid} , followed by a LeakyReLU to introduce nonlinearity. Another linear transformation then adapts the CR by having Γ output features. Finally, the sigmoid activation function is applied to rescale the latent space.

2.2. HyCoT Decoder

The latent space \mathbf{Y} only consists of a few latent channels Γ per pixel. Consequently, a simple feedforward ANN with nonlinear activation functions is sufficient for a qualitative reconstruction. This enables fast decoding for real-time applications or frequent access to data archives with low latency. Thus, similar to the last block on the encoder side, the HyCoT decoder $D_\theta : \mathbf{Y} \rightarrow \hat{\mathbf{X}}$ is lightweight and consists of only a simple MLP with one hidden dimension d_{hid} that upsamples the latent channel dimension Γ back to HSI input bands C . LeakyReLU is used after the initial layer and the sigmoid function after the hidden layer to scale the data back into the range 0–1 for the decoder output. Finally, the decoded pixels are reassembled to form the reconstructed image $\hat{\mathbf{X}}$.

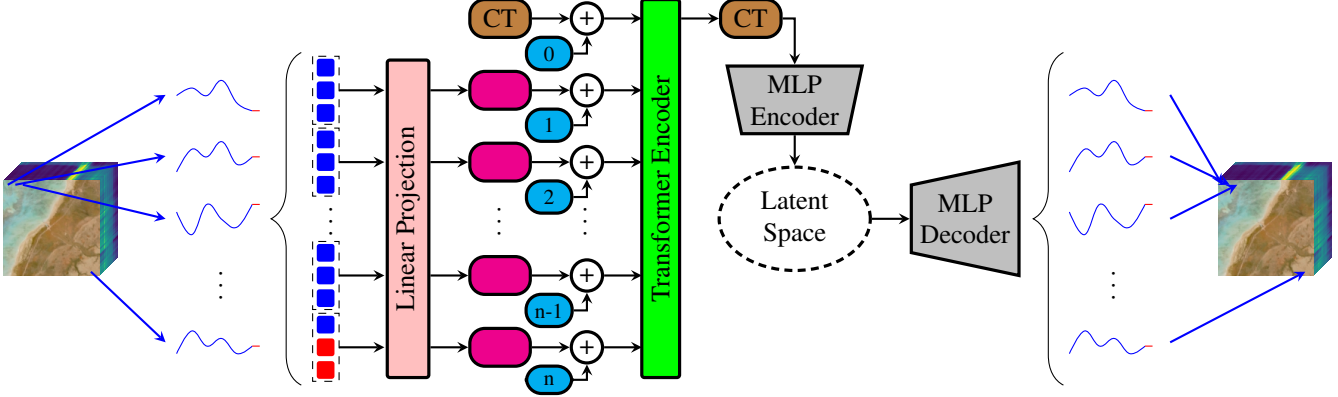


Fig. 1. Overview of our proposed HyCoT model. For each pixel, the spectral signature is padded. Neighbouring spectral bands are grouped and embedded by a linear projection [11] to form the transformer tokens. A CT is prepended and a learned position embedding is added. The sequence of tokens is fed into the transformer encoder [12]. Then, the CT is extracted and projected in the MLP encoder to fit the target CR. An MLP decoder is applied to reconstruct the full spectral signature. Finally, the decoded pixels are reassembled to form the reconstructed HSI.

2.3. Efficient Training Strategy

Data measured by airborne and spaceborne hyperspectral imaging technologies shows spectral similarity among pixels in local spatial regions [15]. This similarity presents redundant information for learning-based pixelwise compression models, including HyCoT. We aim to reduce the training samples within the same HSI by considering only a subset of its pixels. To this end, we propose a random pixel selection strategy within the training HSIs for efficiently reducing the training cost. Instead of using all $W \times H$ pixels of each training HSI $\mathbf{X} \in \mathbb{R}^{H \times W \times C}$, we randomly select pixel subsets of size $w \times h$ in each training epoch with $w \ll W$ and $h \ll H$.

3. EXPERIMENTAL RESULTS

The experiments were conducted on HySpecNet-11k [10] that is a large-scale hyperspectral benchmark dataset based on 250 tiles acquired by the Environmental Mapping and Analysis Program (EnMAP) satellite [16]. HySpecNet-11k includes 11,483 nonoverlapping HSIs, each of them having 128×128 pixels and 202 bands with a ground sample distance of 30 m. Our code is implemented in PyTorch based on the Compress-SAI [17] framework. Training runs were carried out on a single NVIDIA A100 SXM4 80 GB GPU. We used Adam optimizer [18] with a learning rate of 10^{-3} . We trained HyCoT for multiple CRs using mean squared error (MSE) as a loss function until convergence on the validation set, which was achieved after 2,000 epochs for each experiment. For the HyCoT transformer encoder, we used $d_{\text{emb}} = 64$, $L = 5$ and $k = 4$ as suggested in [11]. We empirically fixed the group depth $g_d = 4$ and the hidden MLP dimension of both encoder and decoder to $d_{\text{hid}} = 1,024$.

3.1. Analysis of Training Efficiency

In this subsection, we analyse the efficiency of our proposed training data reduction approach. To this end, we fix $w \times h$ from Subsection 2.3 to have an optimal trade-off between training costs and reconstruction quality. Given the vast number of possibilities, we concentrate on values, where $w = h = 2^n$. In contrast to the training set, the test set is left unchanged to achieve comparable results.

To reduce the computational costs associated with training HyCoT from scratch for each $w \times h$ subset, we employed a new HySpecNet-11k split, denoted as the mini split. The mini split represents a condensed version of HySpecNet-11k, which we recommend to use for hyperparameter tuning. To obtain the mini split, we followed [10] and divided the dataset randomly into i) a training set that includes 70 % of the HSIs, ii) a validation set that includes 20 % of the HSIs, and iii) a test set that includes 10 % of the HSIs. However, the mini split only uses 250 HSIs by extracting the center HSI of each tile used to create HySpecNet-11k. This selection strategy reduces the dataset size by a factor of over 45, while maintaining the global diversity of HySpecNet-11k (11,483 HSIs).

Table 1 shows the results of training HyCoT for the highest considered $\text{CR} = 28.86$ on the HySpecNet-11k mini split using different sizes of randomly sampled pixel subsets (see Subsection 2.3) during training. For this experiment, the HyCoT models were trained for 1,000 epochs with a learning rate of 10^{-4} . The table shows that reconstruction quality can be preserved when training with reduced training pixel subsets. In fact, reconstruction quality for the 16×16 training subset is slightly higher than considering the full 128×128 HSIs. This indicates high redundancy among the pixels within an HSI, suggesting that the entire set of pixels is not necessary to achieve robust generalization performance.

Table 1. HyCoT trained on HySpecNet-11k (mini split) with randomly sampled training subsets for a fixed CR of 28.86. Reconstruction quality is evaluated as PSNR on the test set.

Training Subset Size [pixels]	PSNR [dB]
1 × 1	43.977
2 × 2	44.509
4 × 4	44.886
8 × 8	45.193
16 × 16	45.669
32 × 32	45.344
64 × 64	45.550
128 × 128	45.612

We would like to note that 8×8 , 4×4 and 2×2 pixel subsets can also be considered for even further training cost reduction at a slightly reduced reconstruction quality.

3.2. Rate-Distortion Evaluation

In this subsection, we analyse the rate-distortion curves of learning-based HSI compression models. Our experimental results are shown in Figure 2. To achieve these results, we used the HySpecNet-11k easy split as proposed in [10]. We trained HyCoT, targeting the four specific CRs of 1D-CAE [4], to make our results comparable to the baseline. We would like to note that HyCoT is more versatile in terms of CR, see (7), than CAEs since HyCoT is not based on strided convolutions or pooling operations. For the HyCoT results in Figure 2, we significantly reduced the training costs by a factor of 64 compared to the baseline results by only considering 16×16 pixel subsets in each epoch. Yet, HyCoT is able to outperform all CAE baselines at every CR, which were trained on the full 128×128 HSIs. Quantitatively, HyCoT is at least 1 dB better than 1D-CAE for each CR while for $CR \approx 4$ outperforming SSCNet and 3D-CAE with 13.00 dB and 16.36 dB, respectively. This shows that one-dimensional spectral dimensionality reduction is beneficial for HSI compression and that long-range spectral dependencies, which are captured inside the transformer encoder of HyCoT, are relevant for high quality reconstruction.

3.3. Computational Complexity Analysis

In this subsection, we compare the computational complexity of HyCoT with those of other models. In Table 2 we report a comparison of the floating point operations (FLOPs) and the number of model parameters for multiple CRs. From the table, one can see that for low CRs, 1D-CAE [4] has few parameters. However, by increasing CR, the parameters rise exponentially, since the network stacks up layers with each added downsampling operation. The high FLOPs of 1D-CAE are due to the pixelwise convolutional processing. In con-

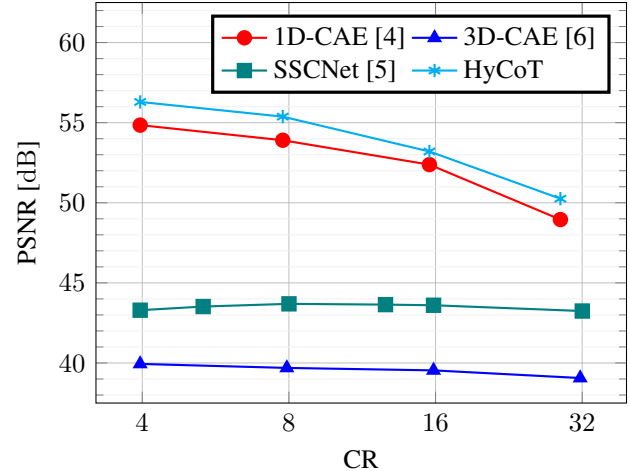


Fig. 2. Rate-distortion performance on the test set of HySpecNet-11k (easy split).

trast, the computational complexity of HyCoT decreases by increasing CRs since the transformer encoder backbone stays the same and only the output channels of the MLP encoder are slimmed, when compressing to a smaller latent space. Thus, HyCoT results in a faster runtime. In addition, increasing the CR reduces the number of parameters compared to 1D-CAE, where the opposite is the case. It is worth mentioning that the lightweight decoder of HyCoT is suitable for real-time HSI reconstruction. We also report the computational complexity for SSCNet and 3D-CAE in the table. SSCNet and 3D-CAE are associated to higher parameter counts and FLOPs due to their multi-dimensional convolutional layers and therefore cannot compete with our HyCoT model.

4. CONCLUSION

In this paper, we have proposed the Hyperspectral Compression Transformer (HyCoT) model. HyCoT compresses hyperspectral images using a transformer-based autoencoder to leverage long-range spectral dependencies. To enhance training efficiency, we have introduced a training strategy that employs only a small, randomized subset of the available training data in each epoch. Experimental results have shown the efficiency of our proposed model in both training time and computational complexity, while also surpassing state-of-the-art convolutional autoencoders in terms of reconstruction quality for fixed compression ratios. As future work, we plan to extend our HyCoT model to achieve efficient spatio-spectral compression.

5. REFERENCES

- [1] S. Lim, K. Sohn, and C. Lee, ‘‘Compression for hyperspectral images using three dimensional wavelet

Table 2. Computational complexity analysis. FLOPs are calculated using a HySpecNet-11k HSI of size 128×128 pixels.

Model	CR	FLOPs	Parameters
1D-CAE [4]	3.96	176.64 G	56,130
SSCNet [5]	4.00	84.18 G	34,136,586
3D-CAE [6]	3.96	121.40 G	933,539
HyCoT	3.96	6.82 G	488,225
1D-CAE [4]	7.77	719.94 G	238,018
SSCNet [5]	8.00	76.56 G	19,240,298
3D-CAE [6]	7.92	104.68 G	677,443
HyCoT	7.77	5.98 G	437,000
1D-CAE [4]	15.54	2,840.00 G	962,242
SSCNet [5]	16.00	72.74 G	11,792,154
3D-CAE [6]	15.84	96.32 G	549,395
HyCoT	15.54	5.54 G	410,363
1D-CAE [4]	28.86	12,180.00 G	3,852,482
SSCNet [5]	32.00	70.84 G	8,068,082
3D-CAE [6]	31.69	92.16 G	485,371
HyCoT	28.86	5.34 G	398,069

transform,” *IEEE International Geoscience and Remote Sensing Symposium*, vol. 1, pp. 109–111, 2001.

- [2] B. Penna, T. Tillo, E. Magli, and G. Olmo, “A new low complexity KLT for lossy hyperspectral data compression,” *IEEE International Symposium on Geoscience and Remote Sensing*, pp. 3525–3528, 2006.
- [3] Q. Du and J. E. Fowler, “Hyperspectral image compression using JPEG2000 and principal component analysis,” *IEEE Geoscience and Remote Sensing Letters*, vol. 4, no. 2, pp. 201–205, 2007.
- [4] J. Kuester, W. Gross, and W. Middelmann, “1D-convolutional autoencoder based hyperspectral data compression,” *International Archives of Photogrammetry, Remote Sensing and Spatial Information Sciences*, vol. 43, pp. 15–21, 2021.
- [5] R. La Grassa, C. Re, G. Cremonese, and I. Gallo, “Hyperspectral data compression using fully convolutional autoencoder,” *Remote Sensing*, vol. 14, no. 10, p. 2472, 2022.
- [6] Y. Chong, L. Chen, and S. Pan, “End-to-end joint spectral–spatial compression and reconstruction of hyperspectral images using a 3D convolutional autoencoder,” *Journal of Electronic Imaging*, vol. 30, no. 4, p. 041403, 2021.
- [7] N. Sprengel, M. H. P. Fuchs, and B. Demir, “Learning-based hyperspectral image compression using a spatio-spectral approach,” *EGU General Assembly*, 2024.
- [8] Y. Guo, Y. Chong, and S. Pan, “Hyperspectral image compression via cross-channel contrastive learning,” *IEEE Transactions on Geoscience and Remote Sensing*, vol. 61, pp. 1–18, 2023.
- [9] A. Altamimi and B. Ben Youssef, “A systematic review of hardware-accelerated compression of remotely sensed hyperspectral images,” *Sensors*, vol. 22, no. 1, p. 263, 2021.
- [10] M. H. P. Fuchs and B. Demir, “HySpecNet-11k: A large-scale hyperspectral dataset for benchmarking learning-based hyperspectral image compression methods,” *IEEE International Geoscience and Remote Sensing Symposium*, pp. 1779–1782, 2023.
- [11] D. Hong, Z. Han, J. Yao, L. Gao, B. Zhang, A. Plaza, and J. Chanussot, “SpectralFormer: Rethinking hyperspectral image classification with transformers,” *IEEE Transactions on Geoscience and Remote Sensing*, vol. 60, pp. 1–15, 2021.
- [12] A. Vaswani, N. Shazeer, N. Parmar, J. Uszkoreit, L. Jones, A. N. Gomez, Ł. Kaiser, and I. Polosukhin, “Attention is all you need,” *Advances in Neural Information Processing Systems*, vol. 30, 2017.
- [13] K. He, X. Zhang, S. Ren, and J. Sun, “Deep residual learning for image recognition,” *IEEE Conference on Computer Vision and Pattern Recognition*, pp. 770–778, 2016.
- [14] J. L. Ba, J. R. Kiros, and G. E. Hinton, “Layer normalization,” *arXiv preprint arXiv:1607.06450*, 2016.
- [15] P. Ghamisi, N. Yokoya, J. Li, W. Liao, S. Liu, J. Plaza, B. Rasti, and A. Plaza, “Advances in hyperspectral image and signal processing: A comprehensive overview of the state of the art,” *IEEE Geoscience and Remote Sensing Magazine*, vol. 5, no. 4, pp. 37–78, 2017.
- [16] L. Guanter, H. Kaufmann, K. Segl, S. Foerster, C. Rogass, S. Chabrillat, T. Kuester, A. Hollstein, G. Rossner, C. Chlebek *et al.*, “The EnMAP spaceborne imaging spectroscopy mission for earth observation,” *Remote Sensing*, vol. 7, no. 7, pp. 8830–8857, 2015.
- [17] J. Bégaint, F. Racapé, S. Feltman, and A. Pushparaja, “CompressAI: A pytorch library and evaluation platform for end-to-end compression research,” *arXiv preprint arXiv:2011.03029*, 2020.
- [18] D. P. Kingma and J. Ba, “Adam: A method for stochastic optimization,” *arXiv preprint arXiv:1412.6980*, 2014.